
This is an electronic reprint of the original article.
This reprint may differ from the original in pagination and typographic detail.

Baniasadi, Hossein; Fathi, Ziba; Cruz, Cristina D.; Abidnejad, Roozbeh; Tammela, Päivi; Niskanen, Jukka; Lizundia, Erlantz

Structure-property correlations and environmental impact assessment of sustainable antibacterial food packaging films reinforced with fungal chitin nanofibrils

Published in:
Food Hydrocolloids

DOI:
[10.1016/j.foodhyd.2024.110987](https://doi.org/10.1016/j.foodhyd.2024.110987)

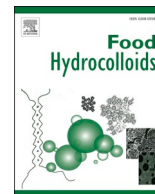
Published: 01/05/2025

Document Version
Publisher's PDF, also known as Version of record

Published under the following license:
CC BY

Please cite the original version:
Baniasadi, H., Fathi, Z., Cruz, C. D., Abidnejad, R., Tammela, P., Niskanen, J., & Lizundia, E. (2025). Structure-property correlations and environmental impact assessment of sustainable antibacterial food packaging films reinforced with fungal chitin nanofibrils. *Food Hydrocolloids*, 162, Article 110987. <https://doi.org/10.1016/j.foodhyd.2024.110987>

This material is protected by copyright and other intellectual property rights, and duplication or sale of all or part of any of the repository collections is not permitted, except that material may be duplicated by you for your research use or educational purposes in electronic or print form. You must obtain permission for any other use. Electronic or print copies may not be offered, whether for sale or otherwise to anyone who is not an authorised user.



Structure-property correlations and environmental impact assessment of sustainable antibacterial food packaging films reinforced with fungal chitin nanofibrils

Hossein Baniasadi ^{a,*}, Ziba Fathi ^b, Cristina D. Cruz ^c, Roozbeh Abidnejad ^b, Päivi Tammela ^c, Jukka Niskanen ^a, Erlantz Lizundia ^{d,e,**}

^a Polymer Synthesis Technology, School of Chemical Engineering, Aalto University, Espoo, Finland

^b Department of Bioproducts and Biosystems, School of Chemical Engineering, Aalto University, FI-00076, Aalto, Finland

^c Drug Research Program, Division of Pharmaceutical Biosciences, Faculty of Pharmacy, University of Helsinki, Pieniäni 5E, 00790, Helsinki, Finland

^d Life Cycle Thinking Group, Department of Graphic Design and Engineering Projects, Faculty of Engineering in Bilbao, University of the Basque Country (UPV/EHU), Bilbao, 48013, Spain

^e BCMaterials, Basque Center for Materials, Applications and Nanostructures, UPV/EHU Science Park, 48940, Leioa, Spain

ARTICLE INFO

Keywords:

Carboxymethylcellulose
Nanochitin
Food packaging
Antibacterial films
Biodegradability
Life cycle assessment

ABSTRACT

This study develops sustainable, antibacterial food packaging films using carboxymethylcellulose and fungi-derived chitin nanofibrils (ChNFs) reinforced with clay to enhance mechanical strength, moisture resistance, and gas barrier properties. ChNFs significantly improve tensile strength and permeability by forming a dense, hydrogen-bonded network within the carboxymethylcellulose matrix. However, excessive ChNF content led to agglomeration, reducing mechanical performance slightly. At 30% ChNFs content, films demonstrated antibacterial activity against *Escherichia coli*, *Staphylococcus aureus*, and *Listeria monocytogenes* and also presented a $52.1 \pm 3.2\%$ degradation rate in four weeks. Life cycle assessment revealed a reduced carbon footprint (5.0–5.3 kg CO₂-equiv. per kg film) and low plastic litter generation (35–44 g/kg), underscoring environmental benefits compared to conventional packaging. These carboxymethylcellulose/ChNF-based films are a promising, eco-friendly alternative for food packaging applications, offering antibacterial properties and enhanced sustainability in the packaging of perishable food products.

1. Introduction

In today's rapidly evolving food industry, food packaging plays a crucial role in ensuring preservation, safety, convenience, and sustainability (Afshar & Baniasadi, 2018; Jurić et al., 2024; Rathee et al., 2024). Traditional petroleum-based packaging materials have raised significant environmental concerns, including plastic pollution, greenhouse gas emissions, and the depletion of finite fossil fuel resources. As a result, there is a growing shift towards biobased, biodegradable, and eco-friendly materials (Basbasan et al., 2022; Molina-Besch & Keszleri, 2023; Ren et al., 2024; Weiland et al., 2024). Among these, cellulose, one of the most abundant organic compounds on Earth, emerges as a promising material for sustainable packaging due to its strength,

resilience, and biodegradability (Baniasadi et al., 2021). Carboxymethylcellulose (CMC), a cellulose derivative, stands out for food packaging applications because of its excellent film-forming properties and biodegradability. However, despite these promising attributes, challenges persist, particularly in enhancing the mechanical strength, moisture resistance, and overall performance of CMC films for packaging applications (Fiori et al., 2019; Fernández-Santos et al., 2022; Liu et al., 2023; Ramakrishnan et al., 2024).

Active food packaging, particularly antibacterial packaging, enhances food safety by reducing microbial contamination, minimizing spoilage, and preventing foodborne illnesses (Mohammadpour Velni et al., 2018; Priyadarshi et al., 2022). Additionally, it helps preserve freshness, sensory appeal, and nutritional value, especially for

* Corresponding author.

** Corresponding author. Life Cycle Thinking Group, Department of Graphic Design and Engineering Projects, Faculty of Engineering in Bilbao, University of the Basque Country (UPV/EHU), Bilbao, 48013, Spain.

E-mail addresses: hossein.baniasadi@aalto.fi (H. Baniasadi), erlantz.lizundia@ehu.eus (E. Lizundia).

<https://doi.org/10.1016/j.foodhyd.2024.110987>

Received 7 October 2024; Received in revised form 30 November 2024; Accepted 13 December 2024

Available online 16 December 2024

0268-005X/© 2024 The Authors. Published by Elsevier Ltd. This is an open access article under the CC BY license (<http://creativecommons.org/licenses/by/4.0/>).

perishable items such as fruits, vegetables, meats, and dairy, thereby reducing food waste and improving economic viability. Several research groups have developed active CMC-based packaging films. For instance, Vargas-Torrico et al. (Vargas-Torrico et al., 2022) developed gelatin-CMC films infused with avocado peel extracts, which demonstrated both antioxidant properties and antifungal activity against *Rhizopus stolonifer* and *Aspergillus niger*. In a subsequent study, Vargas-Torrico et al. (Vargas-Torrico et al., 2024) incorporated pomegranate peel extract into similar films, successfully extending the shelf life of raspberries by 15 days. Sá de Brito et al. (Brito et al., 2023) produced CMC films with propolis extract and titanium dioxide nanoparticles, which enhanced antioxidant activity, improved opacity, and reduced water vapor permeability (WVP). Furthermore, Li et al. (Li, Zhang, et al., 2024) created a multifunctional coating composed of epigallocatechin-3-gallate, cinnamaldehyde, and cysteine in a starch/CMC matrix, which effectively extended the shelf life of strawberries and oranges. Similarly, Tammina et al. (Tammina & Rhim, 2023) developed a CMC/agar film containing nitrogen-doped carbon dots capable of eliminating *Escherichia coli* (*E. coli*) and *Listeria monocytogenes* (*L. monocytogenes*) within 6 h.

In our previous works (Greca et al., 2024; Kramar et al., 2024), we presented a novel and potentially scalable method for producing chitin-based materials with a reduced environmental footprint compared to nanochitin. We demonstrated the potential of fungi-derived chitin nanofibrils (ChNFs) as effective reinforcing fillers in biobased films, highlighting their role in paving the way for sustainable material development beyond nanocellulose. Nanochitin has exhibited significant promise in the biomedical field, particularly for its antibacterial properties (Baharlouei & Rahman, 2022). The antimicrobial effects of chitin are primarily attributed to three mechanisms: the interaction of its cationic groups with the anionic components of bacterial cell membranes, causing leakage of intracellular contents; its low molecular weight, which enhances penetration into the cell nucleus, disrupting RNA and protein synthesis; and its chelating properties, which inhibit bacterial growth (Rabea et al., 2003). However, most studies achieve antimicrobial activity by incorporating natural products or essential oils into ChNF films (Heydarian & Shavisi, 2023; Khazaei et al., 2024). A notable exception is the work by Mei-Chun Li et al. (Li et al., 2016), who demonstrated that ChNFs alone effectively inhibited the growth of the gram-negative bacterium *E. coli*, though they showed a lesser effect against the gram-positive bacterium *Staphylococcus aureus* (*S. aureus*). Despite these promising findings, its application in food packaging materials remains underexploited. This study hypothesizes that ChNFs, when integrated into CMC films, will enhance their mechanical, moisture barrier, and antibacterial properties, thereby providing a sustainable and functional solution for food packaging.

To test this hypothesis, we incorporated varying concentrations of ChNFs into CMC-based films and evaluated their mechanical properties, permeability, antibacterial activity, and biodegradability. Additionally, a life cycle assessment (LCA) was conducted to assess the environmental impact of the films, including their carbon footprint and potential for plastic waste generation. The strategy to address these identified challenges involved a detailed structure-property correlation analysis to understand how ChNFs influence film performance, paired with a focus on sustainability through LCA. Our findings indicate that these CMC/ChNF-based films are a functional and sustainable alternative to conventional food packaging, supporting eco-friendly and bioactive packaging solutions and advancing sustainability in the food industry.

2. Experimental

2.1. Materials

Carboxymethylcellulose sodium salt (CMC, average molecular weight of 250,000 g/mol, degree of substitution of 0.7) and glycerol (purity: >99.0%, GC) were purchased from Tokyo Chemical Industry

Co. Citric acid monohydrate (CA), sodium montmorillonite clay (Na-MMT), sodium hydroxide (NaOH) pellets (99%), and sodium hypophosphite (SHP, 99%) were obtained from Sigma-Aldrich. Fresh and mature (round cap, intact veil, long stem) *Agaricus bisporus* (white button mushrooms) were sourced from a local store in Bilbao, Spain. Clinical bacterial strains, including *E. coli* ATCC 25922 and *S. aureus* ATCC 29213, were acquired from Microbiologics Inc. (St. Cloud, Minnesota, USA). *L. monocytogenes* DSM 112142 (isolated from minced meat) was obtained from the Leibniz Institute DSMZ German Collection of Microorganisms and Cell Culture. Cefaclor antimicrobial susceptibility discs (30 µg) were purchased from Thermo Fisher Scientific through Oxoid Ltd, Hampshire, UK.

2.2. Nanochitin isolation and characterization

ChNF was extracted from *Agaricus bisporus* using a top-down method (Ruiz et al., 2023; Nawawi et al., 2019). Frozen mushrooms (−8 °C, for one week) were first immersed in distilled water at a 1:2 ratio for 5 min and then washed four times to remove dirt and debris. The cleaned mushrooms were blended for 5 min using a Power Black Titanium 1800 blender (13000 rpm). The resulting mixture was heated at 85 °C for 30 min, with the reaction quenched by adding five times the volume of cold distilled water. After centrifugation, the pellet was collected and redispersed in distilled water. Next, 1 M NaOH was then added to the mixture, which was heated at 65 °C for 180 min with stirring. Following this step, the mixture was additionally blended for 1 min. Finally, the mixture was dialyzed against distilled water (molecular weight cut-off of 12–14 kDa) for one week before use.

The powder X-ray diffraction (XRD) pattern of nanochitin was recorded using a D8 Discover diffractometer with Cu K α radiation (45 kV, 40 mA) in reflection mode. Fourier transform infrared (FTIR) spectroscopy was conducted in attenuated total reflection (ATR) mode using a Jasco FT/IR-6100 spectrometer equipped with a diamond ATR accessory, covering the 3600–800 cm^{−1} range with a 2 cm^{−1} resolution. Carbon nuclear magnetic resonance (¹³C NMR) spectroscopy was performed at room temperature on a Bruker Avance DPX 300 (Bruker, USA) operating at a 75.5 MHz resonance frequency. The NMR spectra were acquired using an inverse gated decoupled sequence with a 3 s acquisition time, 4 s delay time, 5.5 µs pulse, spectral width of 18800 Hz, and more than 10,000 scans. The degree of acetylation (DA) was calculated using the following equation (Heux et al., 2000):

$$DA (\%) = \frac{6 \times I_{CH_3}}{I_{C_1-C_6}} \times 100 \quad (1)$$

where I_{CH_3} represents the integral of the methyl peak, and $I_{C_1-C_6}$ accounts for the sum of all the carbon atoms in the D-glucopyranosyl ring. The morphology of nanochitin was examined using transmission electron microscopy (TEM) on a JEOL JEM 1400 Plus apparatus with an acceleration voltage of 100 kV. A 3 µL droplet of a 0.01 wt% aqueous dispersion was deposited onto a hydrophilic EMS CF300-Cu grid (treated with glow discharge at 10 mA for 30 s in a Leica EM ACE200) and stained with 1% uranyl acetate for 20 s.

2.3. Film preparation

Pure CMC film was prepared by dissolving 1.5 g of CMC in distilled water at room temperature for 24 h. Glycerin, at 25% of the dry mass of CMC, was added as a plasticizer. Additionally, CA at 10% of the dry mass of CMC was introduced as a crosslinking agent, and a small amount of SHP was added as a catalyst. The mixture was stirred for 1 h and then left to rest for another hour to remove any formed bubbles. The solution was then cast into a Petri dish and dried at ambient temperature for 24 h. The dried film was subsequently placed in an oven at 70 °C for 5 min to complete the crosslinking process.

For the clay-containing film, a prescribed amount of clay was first

dispersed in water using 30 min of sonication, followed by 30 min of stirring at room temperature. After this, the CMC was introduced. The remainder of the fabrication process followed the same as the method described for the pure CMC film. Based on the results of our previous study (Baniasadi et al., 2024), the clay content in the film was fixed at 3% (w/w) since it provided the optimum properties. This sample was designated as CMCC.

For the fabrication of ChNF-containing films, the ChNF mixture was diluted to 1.5%. Next, different concentrations of ChNF were added to the CMC/clay mixture. The remainder of the fabrication process followed the same as that described for the pure CMC film. The concentration of each component, as well as the codes for the films, are listed in Table 1.

2.4. Film characterizations

2.4.1. Morphological analysis of the composite films

The morphology of the films was investigated through scanning electron microscopy (SEM) on cryofractured surfaces using a Zeiss Sigma VP. SEM imaging was performed at a voltage of 3 kV, with the surface coated with a thin layer of gold prior to scanning. The surface morphology of the films before and after the degradation test was also assessed using SEM imaging.

2.4.2. Evaluation of film transmittance properties

The transmittance properties of the film were evaluated using a UV-3100 PC spectrophotometer (Shimadzu, Japan) at 23 °C, with scanning performed across the visible spectrum (400–700 nm). Special attention was given to the transmittance at 600 nm. Each film sample was cut into a rectangular piece measuring 3 cm × 0.5 cm and was directly affixed to the cuvette wall for testing. Transparency (%) was determined using Equation (2), where T_1 denotes the incident light intensity from the spectrophotometer source before it passes through the blank sample (100%), and T_2 represents the transmitted light intensity through the film as:

$$\text{Transparency (\%)} = \frac{T_2}{T_1} \times 100 \quad (2)$$

2.4.3. Assessment of mechanical properties

The mechanical properties of the film were evaluated using a tensile test performed on a Universal Tester Instron model 4204. The samples were stretched under a 1 kN load cell at a rate of 5 mm/min. Testing was conducted at 23 °C, with samples conditioned for 48 h at a temperature of 23 °C and a humidity level of 55%. Typical stress-strain curves were plotted, and relevant data—including tensile modulus, tensile strength, and elongation at break—were extracted and analyzed. Each measurement was repeated five times, and the mean value ± standard deviation was reported.

Table 1
Composition and codes of the prepared films.

Sample	CMC ^a (mL)	ChNF ^a (mL)	Clay (g) >	Glycerin (g)	CA (g)	SHP (g)
CMC	100	0	0	0.375	0.15	0.015
CMCC	100	0	0.045	0.375	0.15	0.015
CMCC- NC5	95	5	0.045	0.375	0.15	0.015
CMCC- NC10	90	10	0.045	0.375	0.15	0.015
CMCC- NC20	80	20	0.045	0.375	0.15	0.015
CMCC- NC30	70	30	0.045	0.375	0.15	0.015

^a The concentration is 1.5% (w/w).

2.4.4. Evaluation of oxygen and water vapor permeability

Oxygen transmission rate (OTR) tests were conducted in line with ASTM D 3985-95 standards at 23 °C and 50% relative humidity, using a Mocon Oxtran 2/22 L Oxygen Permeability Analyzer (Mocon, Minneapolis, USA). Samples with an area of approximately 5.5 cm² were exposed to an oxygen partial pressure of 1 atm. To calculate the oxygen permeability, the OTR was normalized by taking into account the sample area, oxygen pressure, and material thickness.

WVP was measured following ASTM D1653 using TQC Sheen Permeability Cups. Initially, a disk-shaped sample was dried in a vacuum oven at 60 °C for 24 h. The dried sample was then weighed (m_0) and placed into a permeability cup containing a specific amount of dried silica gel. The cup with the sample was positioned in a controlled humidity chamber set to 60% relative humidity at 23 °C. Over a 48-h period, the weight changes of the cup (Δm) were carefully monitored. A plot of Δm (g) versus time (h) was created, and a linear curve was fitted to the data. The slope of this curve (g/h) was then used to calculate the WVP (g·m/m²·Pa/h) according to Equation (3) as:

$$\text{WVP} = \frac{\Delta m \times d}{t \times A \times \Delta P} \quad (3)$$

Here, d denotes the film thickness (m), A represents the area of the film through which water vapor is transmitted (0.001 m²), and ΔP corresponds to the saturated vapor pressure at 25 °C (3170 Pa).

2.4.5. Surface wettability and contact angle measurements

The surface wettability of the sample was evaluated by determining the static contact angle of a water droplet with a Theta Flex Optical Tensiometer. A 5 µL water droplet was placed on the surface, and the contact angle was recorded both immediately after deposition and after 60 s. The reported contact angles represent the average of at least three separate measurements.

2.4.6. Soil burial degradation testing

The degradation of the sample was examined through a soil burial experiment using Biolan garden black soil. Initially, the sample was dried in a vacuum oven at 60 °C for 24 h to eliminate any moisture. After drying, the sample was weighed (m_0) and then buried in the soil. This experiment was conducted in late winter, specifically in January 2024. During the conditioning period, the soil beds were regularly watered and mixed to maintain consistent moisture levels. Each week, the sample was removed, its surface was cleaned with blotter paper, and it was reweighed (m_i). The degradation rate (D) was subsequently calculated using Equation (4):

$$D(\%) = \frac{m_0 - m_i}{m_0} \times 100 \quad (4)$$

2.4.7. Antibacterial assessment

All bacterial strains were stored at −80 °C, with working cultures maintained on Mueller Hinton Agar (MHA) plates at 2–8 °C. The antibacterial properties of the films were evaluated using the Kirby-Bauer disk diffusion method (CLSI M02-A12 and CLSI M100-S26, 2015). Pre-cut round discs of the films (approximately 7 mm in diameter) were sterilized under UV light for 15 min. Fresh bacterial cultures were grown on MHA plates at 37 °C for 16–20 h prior to the assay. A few colonies from the overnight culture were inoculated into 0.9% saline solution and vortexed to ensure homogeneity. The bacterial suspensions were standardized to a 0.5 McFarland standard using a DEN-1 densitometer (BioSan), corresponding to approximately 1.2×10^8 colony-forming units (CFU/mL). A sterile cotton swab was dipped into the bacterial suspension and evenly spread across three replicate MHA plates per bacterial strain. Sterile forceps were used to apply the film discs to the agar surface, and they were gently pressed into place. The plates were incubated at 37 °C for 24 h. Cefaclor (30 µg) was used as a positive control, while CMC and CMCC films served as negative controls on each

assay plate. The zones of growth inhibition were measured using a caliper (in mm), subtracting the size of the discs from the final measurements. Average values were reported. Initial screening experiments were performed once in triplicate. For films that exhibited antibacterial activity (i.e., a zone of inhibition), experiments were repeated twice more, each in triplicate.

2.4.8. Statistical analysis

Statistical analysis was performed using OriginPro Graphing and Analysis software, version 2021b (OriginPro). Analysis of Variance (ANOVA) was used to compare the means of different groups. Where applicable, post-hoc tests were conducted to assess differences between groups. Differences were considered statistically significant at $p < 0.05$. All data are presented as mean \pm standard deviation.

2.5. Life cycle assessment

The LCA methodology, in accordance with ISO 14040/44 international standards (Laurent et al., 2020), was employed to evaluate the cradle-to-gate environmental impacts of the developed materials. This assessment encompasses the acquisition of raw materials, their upstream processes, transportation to the factory gate, energy requirements for in-situ processing, and waste management. The life cycle inventory (LCI) was derived from primary data obtained through our laboratory experiments. For ChNF extraction, white button mushrooms were considered to have no associated burden, which is in line with cut-off allocation principles. However, a 100 km transport distance from the farm to the factory gate was included to account for impacts during processing. Energy demand was extrapolated based on equipment power and usage time, with a 70% load factor. Medium-voltage electricity from renewable sources was used to reflect the transition of the energy mix around the globe. The complete LCI is detailed in Tables S1–S3 for future reference and comparisons. The impact assessment has been performed

using OpenLCA version 2.2.0 (available as of June 20, 2024). Three different methodologies have been implemented to complete the assessment. First, the cumulative energy demand (CED) and ReCiPe 2016 v1.03, Midpoint (H) methodologies have been applied using the "ecoinvent v3.10 Cut-Off Unit Processes" database. Next, the "ecoinvent v3.10 APOS Unit-Processes PLEX" database was used to estimate the amount of plastic litter generated. 1 kg of processed film has been defined as the functional unit (FU). The details of the methodologies, their implementation, and underlying assumptions are explained in the Supplementary Information, Section S1.

3. Results and discussion

3.1. Nanochitin characterizations

ChNF was isolated from white button mushrooms (*Agaricus bisporus*) by alkaline treatment (1 M NaOH) assisted by mild mechanical fibrillation in a conventional kitchen blender (Ruiz et al., 2023; Nawawi et al., 2019). The chemical structure and morphology of the isolated ChNF were investigated to confirm the successful extraction and preservation of the nanofibrils' intrinsic properties. The XRD pattern shown in Fig. 1a reveals the semicrystalline nature of the isolated ChNF, indicated by two prominent diffraction peaks superimposed on an amorphous background. These peaks, located at $2\theta = 9.2^\circ$ and 20.1° , correspond to the (020) and (110) crystallographic planes of α -chitin, respectively, consistent with its known crystalline structure (Zhang et al., 2005).

The FTIR spectrum in Fig. 1b further supports the chemical integrity of ChNFs. A broad absorption band between 3650 and 3200 cm^{-1} is attributed to the stretching vibrations of hydroxyl ($-\text{OH}$) and amine ($-\text{NH}$) groups. Two additional peaks at 2911 and 2841 cm^{-1} correspond to the asymmetrical and symmetrical stretching vibrations of methyl and methylene groups. The characteristic amide bands of chitin appear

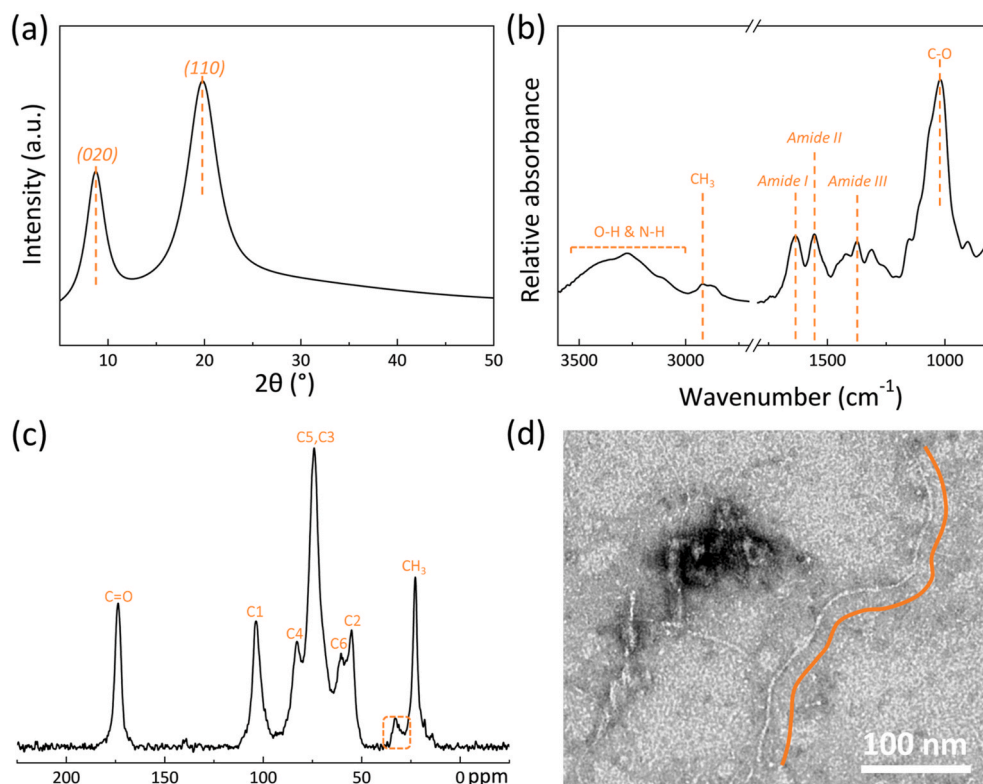


Fig. 1. ChNF characterization: (a) XRD, (b) ATR-FTIR, (c) ^{13}C NMR, and (d) TEM. The presence of amorphous β -glucans is highlighted with a dotted rectangle in part (c). The shape of an individual nanofiber is marked in orange in part (d). (For interpretation of the references to colour in this figure legend, the reader is referred to the Web version of this article.)

at 1628 cm^{-1} (Amide I), 1556 cm^{-1} (Amide II), and 1315 cm^{-1} (Amide III), confirming the presence of chitin's acetamido groups. A band at 1030 cm^{-1} corresponds to C–O stretching, further verifying the molecular structure (Duarte et al., 2002). The solid-state ^{13}C NMR in Fig. 1c displays the characteristic carbon peaks associated with α -chitin, including those from the carbonyl group (C=O) and the six carbons of the glucosamine backbone (C₁ to C₆), along with the methyl group of the N-acetyl group (CH₃). The degree of N-acetylation, calculated using Equation (1), is estimated to be 77%, indicating a high level of acetylation typical of α -chitin (Kasaai, 2010). A small peak at ~ 33 ppm (highlighted with a dotted rectangle) suggests the presence of amorphous β -glucans, which remain covalently bound to the ChNF, possibly originating from the mushroom cell walls (Espartero et al., 2023). Morphological observations using TEM, shown in Fig. 1d, confirm the nanofibrillar and flexible nature of the isolated ChNF.

The nanofibrils exhibit a smooth surface, with lengths ranging from 100 to 500 nm and diameters below 10 nm. Serving as a structurally important component of the fungal cell wall, these observations suggest that nanochitin is formed through the aggregation of stretched chitin macromolecules. Additionally, surface charge characterization using zeta-potential measurements, shown in Fig. S1, reveals a slightly positive charge at low pH ($\sim +7$ mV at pH 2), resulting from the protonation of the N-acetyl groups in chitin. The zeta potential gradually becomes more negative with increasing pH. A comparison with nanochitin derived from crustacean exoskeletons (isolated through HCl-assisted hydrolysis) reveals more negatively charged surfaces for ChNFs, suggesting a reduced amount of amine groups on the nanochitin (Espartero et al., 2023).

3.2. Structure-property correlations

3.2.1. Morphology and microstructure study

The SEM images were used to examine the morphology and fracture surface characteristics of the pure CMC film and the composite films incorporating clay and ChNFs (Fig. 2). The fracture surface of the pure CMC film appeared smooth, dense, and uniform, with no visible pores or cracks, indicating a homogeneous structure with minimal internal defects (Fig. 2a). The incorporation of clay resulted in a slightly more irregular and rougher surface, which can be attributed to the increased

stiffness and rigidity imparted by the clay particles. However, the surface maintained a high degree of smoothness, suggesting good compatibility between the components and no evidence of phase separation, as evidenced in Fig. 2b (Khezriani & Shahbazi, 2018; Wang et al., 2024). The addition of ChNF further modified the surface, leading to more pronounced fracture patterns and a noticeable decrease in smoothness (Fig. 2c–f). No signs of ChNFs were observed on the fractured surfaces. This can be attributed to the similar secondary electron signals in the SEM images for both CMC and ChNFs, as they are organic materials with relatively comparable electron densities and atomic compositions. Furthermore, the images suggest that the ChNFs remain well distributed within the CMC matrix without aggregation. In fact, ChNF likely served as a reinforcing agent, enhancing interfacial bonding between the CMC matrix and the clay particles. This improved interface may have contributed to a more energy-absorbing fracture mechanism, as reflected by the increased roughness and tortuosity of the fracture surface (Sun et al., 2024). Notably, none of the composite films showed visible cracks, signifying that the components were homogeneously dispersed and demonstrated excellent compatibility (Alshehri et al., 2024).

3.2.2. Transparency analysis

The transparency and transmittance properties of food packaging films are crucial for both their visual appeal and functional performance, particularly in protecting light-sensitive products from UV degradation (Basbasan et al., 2022; Ren et al., 2024). The transparency of the films was measured at 600 nm, and UV transmittance was assessed across the 200–800 nm range (Fig. 3a–c). The pure CMC film exhibited a transparency level of $79.67 \pm 2.21\%$, consistent with previous studies (Fernández-Santos et al., 2022). When 3% (w/w) clay was incorporated into the CMC matrix (CMCC film), a slight reduction in transparency was observed, attributed to light scattering by the clay particles (El Mouza-him et al., 2023a). Incorporating ChNF further decreased transparency, with the CMCC-NC30 film showing the greatest reduction ($31.03 \pm 1.14\%$), likely due to increased light scattering from the ChNF particles (Subramani & Manian, 2024). The UV–Vis spectra, on the other hand, revealed that higher ChNF concentrations enhanced UV-blocking properties. While the pure CMC and CMCC films showed moderate UV transmittance, the CMCC-NC series exhibited progressively lower

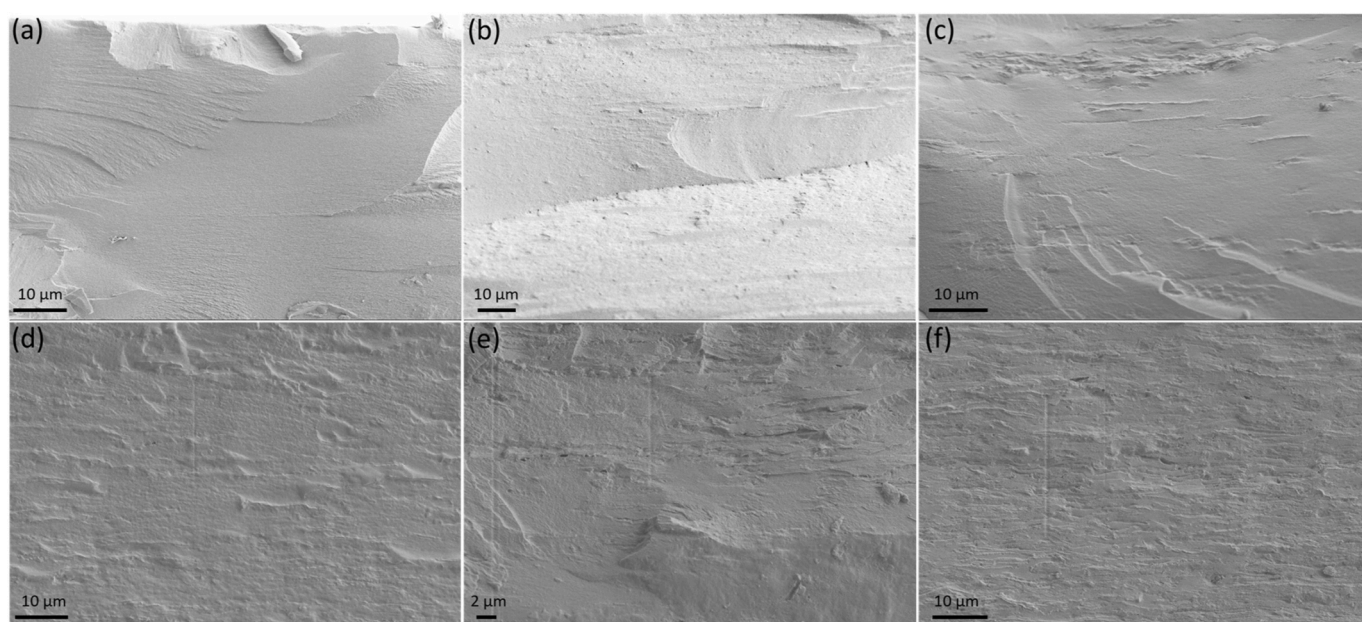


Fig. 2. SEM micrographs of pure CMC film and composite films with clay and ChNF: (a) CMC, (b) CMCC, (c) CMCC-NC5, (d) CMCC-NC10, (e) CMCC-NC20, and (f) CMCC-NC30. The images were captured from the fracture surface area.

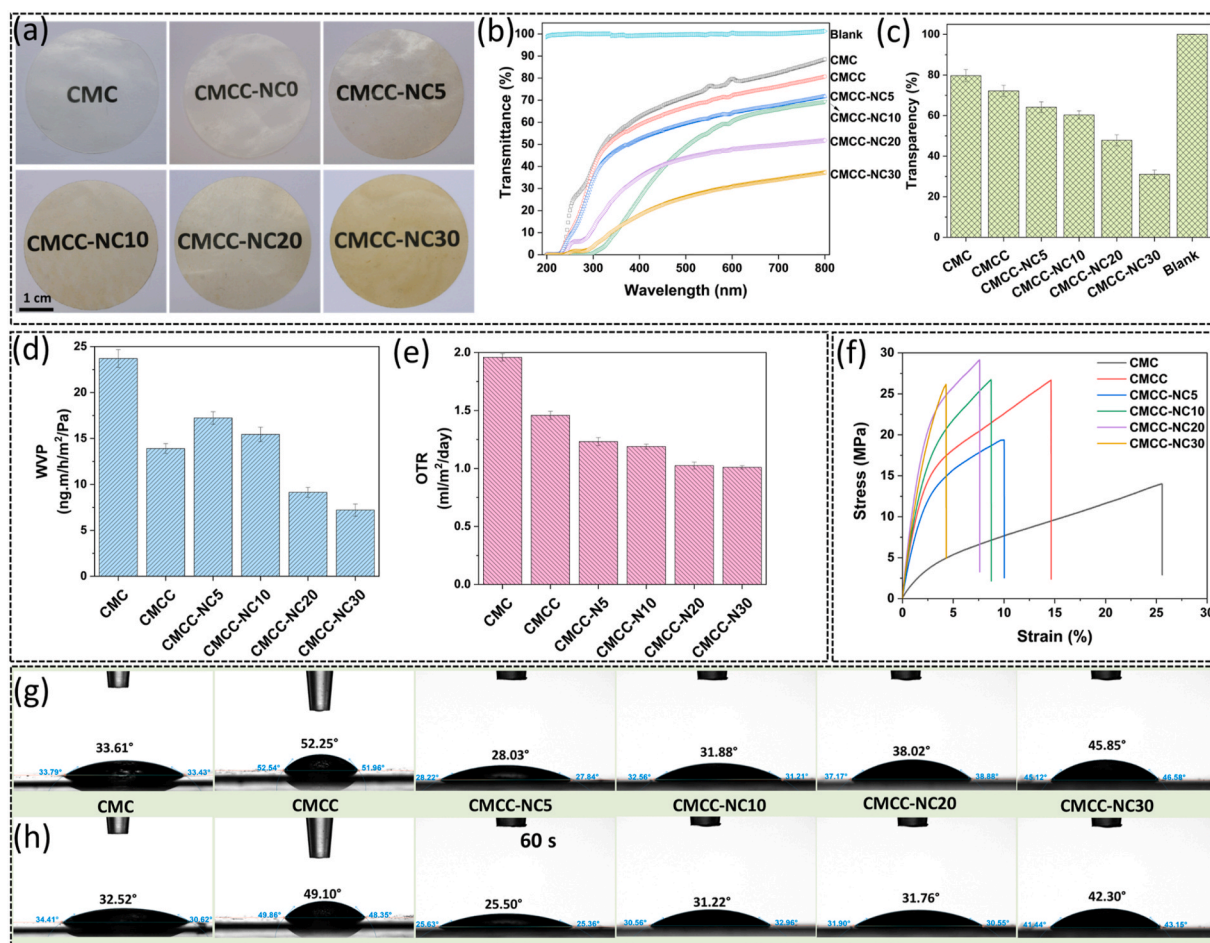


Fig. 3. (A) Digital photograph of the fabricated films. (b) UV-Vis spectra of the films, scanned from 400 to 700 nm at 23 °C. (c) Transparency of the films measured at 23 °C and 600 nm. (d) WVP and (e) OTR results at 23 °C. (f) Typical stress-strain curves from tensile testing. (g) Water contact angle measurement 10 s after droplet deposition at 23 °C. (h) Water contact angle measurement 60 s after droplet deposition at 23 °C. Representative images are provided.

transmittance, with CMCC-NC30 providing the most effective UV protection. This enhanced UV-blocking ability is a beneficial feature for food packaging, protecting sensitive products from UV degradation (Alkassfarity et al., 2024; Halloub et al., 2024).

3.2.3. Permeability measurements: oxygen and water vapor

The permeability to oxygen and water vapor is crucial for assessing food packaging materials' barrier properties, which affect shelf life and food quality (Ganjeh et al., 2024; Jahangiri et al., 2024). The WVP and OTR of the fabricated films were measured and are summarized in Fig. 3d and e. Initial tests on the pure CMC film showed baseline values for WVP (23.70 ± 0.97 ng m/h·m²·Pa) and OTR (1.96 ± 0.03 mL/m²·day), consistent with the literature (Li et al., 2024; Priyadarshi et al., 2021; Rezaei et al., 2023). Incorporating 3% clay into the CMC matrix (CMCC film) reduced permeability, with WVP and OTR decreasing by 40% and 25%, respectively. This reduction, which was observed by other researchers (Mao et al., 2023; Subramani & Manian, 2024), is attributed to the formation of a more compact network, where clay particles create a tortuous path that impedes gas and vapor diffusion (Dairi et al., 2019; El Mouzahim et al., 2023a). Moreover, the high aspect ratio of the clay particles improves interaction with the CMC matrix, reinforcing the overall structure and enhancing its impermeability.

The addition of ChNF further improved the permeability properties. For instance, the CMCC-NC30 film (with 30% ChNF) exhibited the lowest WVP (7.21 ± 0.26 ng m/h·m²·Pa) and OTR (1.01 ± 0.01 mL/m²·day). The reinforcing effect of ChNF, along with its strong

interactions with the CMC-clay matrix—such as hydrogen bonding, van der Waals forces, and electrostatic interactions—promotes better particle distribution and dispersion throughout the film, further contributing to the reduction in permeability. Notably, the observed WVP and OTR values fall within the effective range for food packaging, particularly for oxidation-sensitive products (Coles et al., 2003; Robertson, 2009).

3.2.4. Mechanical properties evaluation

Evaluating the mechanical properties of food packaging materials is essential for assessing their durability and flexibility under various conditions. In this study, tensile strength, modulus, and elongation at break were measured, with results summarized in Fig. 3f and Table 2.

Table 2
Mechanical properties of the films extracted from stress-strain curves.

Sample	Tensile modulus (MPa)	Tensile strength (MPa)	Elongation at break (%)
CMC	154 ± 9 ^a	14.0 ± 0.7	25.6 ± 1.3
CMCC	840 ± 17	26.8 ± 0.9	14.6 ± 0.7
CMCC-NC5	685 ± 11	19.5 ± 1.2	10.0 ± 0.9
CMCC-NC10	915 ± 35	26.7 ± 0.9	8.7 ± 0.4
CMCC-NC20	1120 ± 78	29.2 ± 1.1	7.6 ± 0.6
CMCC-NC30	1033 ± 45	26.3 ± 0.8	4.3 ± 0.2

^a Averages (± standard deviation) were calculated from three experiments conducted in triplicate.

The pure CMC film showed baseline values for tensile strength (14 ± 0.7 MPa), tensile modulus (154 ± 9 MPa), and elongation at break ($25.6 \pm 1.3\%$), consistent with previous studies (Fiori et al., 2019; Shan et al., 2024a). Incorporating 3% clay (CMCC film) significantly improved tensile strength (26.8 ± 0.9 MPa) and modulus (840 ± 17 MPa) but reduced elongation at break to $14.6 \pm 0.7\%$. The enhanced mechanical properties are attributed to the clay particles reinforcing the film structure, although the increased rigidity resulted in reduced flexibility. While similar improvements in tensile strength and modulus have been noted in some studies (Hou et al., 2024; Majumder et al., 2023), other reports have observed reductions in tensile strength following the incorporation of clay (El Mouzahim et al., 2023a; Mohsen et al., 2024; Subramani & Manian, 2024), likely due to low interactions between the clay and polymer matrix.

As provided in Table 2, the addition of ChNF to the CMCC composite initially decreased tensile strength and modulus at lower concentrations, but these values increased significantly with higher ChNF content. For example, the CMCC-NC20 film showed tensile strength (29.2 ± 1.1 MPa) and modulus (1120 ± 78 MPa), which were higher than that of the CMCC film. At the highest ChNF concentration (CMCC-NC30), a slight reduction in properties was observed, likely due to particle agglomeration, which disrupted the film's structure. The improved mechanical performance suggests enhanced compatibility between the filler and matrix, likely due to better hydrogen bonding and interfacial adhesion. Furthermore, as CMC is a negatively-charged water-soluble polyelectrolyte, and ChNFs are positively charged, electrostatic interactions may appear between the matrix and the filler. This stronger adhesion at higher concentrations allows for more effective stress transfer between the ChNF and the CMC matrix, reinforcing the composite structure. Oun et al. (Oun & Rhim, 2017a, 2017b) reported that incorporating chitin nanowhiskers into CMC enhanced its mechanical properties. Notably, a 10% (w/w) addition resulted in significant enhancements, including an 88% increase in tensile strength and a 243% increase in elastic modulus. Similar enhancements were noted in other studies, with chitin nanocrystals increasing the tensile strength of CMC by 19.7% and stiffness by 58.7% (Oun & Rhim, 2020).

3.2.5. Study of surface wettability

Surface wettability is crucial for food packaging materials, as it affects moisture interaction, barrier properties, and overall durability. The water contact angle is used to assess wettability, with lower angles indicating higher hydrophilicity. Photographs of the deposited droplet at 10 s and 60 s after deposition, along with the corresponding average water contact angles at each time point (mean value of the angles observed on both the left and right sides of the droplet), are shown in Fig. 3g and h. The pure CMC film exhibited a contact angle of approximately 34° , indicating a relatively hydrophilic surface, aligning with the inherent hydrophilic nature of cellulose, which tends to absorb moisture and interact readily with water (Yang et al., 2024). Incorporating 3% (w/w) clay increased the contact angle to 52° , suggesting reduced wettability. This can be attributed to the formation of a more compact and less porous film through hydrogen bond interactions, reducing the availability of hydrophilic sites on the surface. Furthermore, clay, with its layered structure, can effectively alter the surface energy, making the composite films less prone to moisture absorption (Yin et al., 2024). However, contrary to our observations, Gasti et al. (Gasti & Dixit, 2024) reported that the water contact angle of polyvinyl alcohol films decreased with the addition of clay particles, attributed to an increase in surface roughness.

The addition of ChNF to the CMCC composite showed a complex effect on wettability. At 5% (w/w) ChNF, the contact angle decreased to 28° , suggesting enhanced hydrophilicity. However, as the ChNF content increased, the contact angle rose, reaching approximately 32° at 10%, 38° at 20%, and 46° at 30%. The initial slight reduction in contact angle at lower concentrations may be due to surface roughness effects. In contrast, the subsequent increase in contact angle is likely explained by

the presence of hydrophobic hydrophobins, which are hydrophobic proteins in ChNFs (Azpitarte Aretxabaleta et al., 2024). At higher concentrations, these hydrophobic components could dominate the surface properties, reducing interaction with water and creating a more hydrophobic surface. It should be highlighted that the observed contact angle for the films, even with the presence of clay particles and ChNFs, still indicates higher hydrophilicity and a stronger affinity to water, which may result in spoilage of packaged foods. However, the films require further optimization. They can still be suitable for packaging products that are less sensitive to water, such as dry foods or non-perishable items.

3.2.6. Soil burial degradation testing

Soil burial degradation tests assess the biodegradability of food packaging materials, providing insights into their environmental impact post-use. This test mimics real-world conditions, providing insight into the breakdown of materials under microbial activity in soil (Mishra et al., 2024). In this study, the degradation rate of the films was measured over four weeks, with results summarized in Table 3. The pure CMC film showed significant degradation, with a 50.5% weight loss by week 4, consistent with its relatively hydrophilic nature, which facilitates microbial breakdown (Dong et al., 2024; Shan et al., 2024b). Incorporating 3% (w/w) clay (CMCC) reduced degradation to 37.3%, attributed to the structural reinforcement provided by the clay particles, which creates a more compact matrix and reduces water absorption (Bangar et al., 2023). This trend is consistent with other studies where the addition of inorganic fillers reduced the rate of biodegradation due to the less permeable and more rigid composite structure (Kaur et al., 2024; Yin et al., 2024). However, in contrast to our results, some researchers reported that the addition of kaolin clay increased the degradation rate of chitosan films, attributing this effect to the solubility and reduced mechanical and antioxidant properties of the film (El Mouzahim et al., 2023b; Gülpınar et al., 2024; Subramani & Manian, 2024).

At lower concentrations of ChNFs (5%), the degradation rate was slightly lower than that of CMCC, reaching 40.8% by week 4. As ChNF content increased, the degradation rate improved, with the CMCC-NC30 composite showing a 52.1% weight loss by week 4. This suggests that ChNF enhances the film's biodegradability. The increased biodegradation observed with nanochitin, as reported by other researchers (Kim et al., 2024; Motloung et al., 2024; Sagaya Deva Niranjana & Krishnamoorthy, 2024), may be due to the formation of a more porous structure, which facilitates microbial penetration. Additionally, at higher concentrations, ChNFs may aggregate, creating microdomains that facilitate microbial penetration despite the increased hydrophobicity observed in the contact angle measurements, thereby accelerating degradation. Both chitin and ChNF are non-toxic to humans and the environment, offering a sustainable alternative to synthetic materials and contributing to the reduction of harmful chemicals and pollutants released into ecosystems (Ngasotter et al., 2023).

The SEM images taken before and after the soil burial degradation test were used to examine the morphological changes in the films, as shown in Fig. 4. Additionally, digital photographs of the degraded samples are also presented in Fig. 4. Prior to degradation, the surface of

Table 3
Soil burial degradation test results for four weeks.

Sample	Week 1 (%)	Week 2 (%)	Week 3 (%)	Week 4 (%)
CMC	33.6 ± 1.4^a	40.8 ± 2.1	46.7 ± 1.8	50.5 ± 3.1
CMCC	17.3 ± 0.7	22.6 ± 1.2	27.2 ± 1.0	37.3 ± 2.4
CMCC-NC5	25.7 ± 1.0	30.9 ± 1.6	35.7 ± 1.4	40.8 ± 2.5
CMCC-NC10	28.9 ± 1.2	32.4 ± 1.7	35.2 ± 1.4	40.2 ± 2.5
CMCC-NC20	29.2 ± 1.2	33.9 ± 1.8	38.0 ± 1.5	48.2 ± 2.9
CMCC-NC30	41.5 ± 1.7	45.3 ± 2.4	49.1 ± 2.0	52.1 ± 3.2

^a Averages (\pm standard deviation) were calculated from three experiments conducted in triplicate.

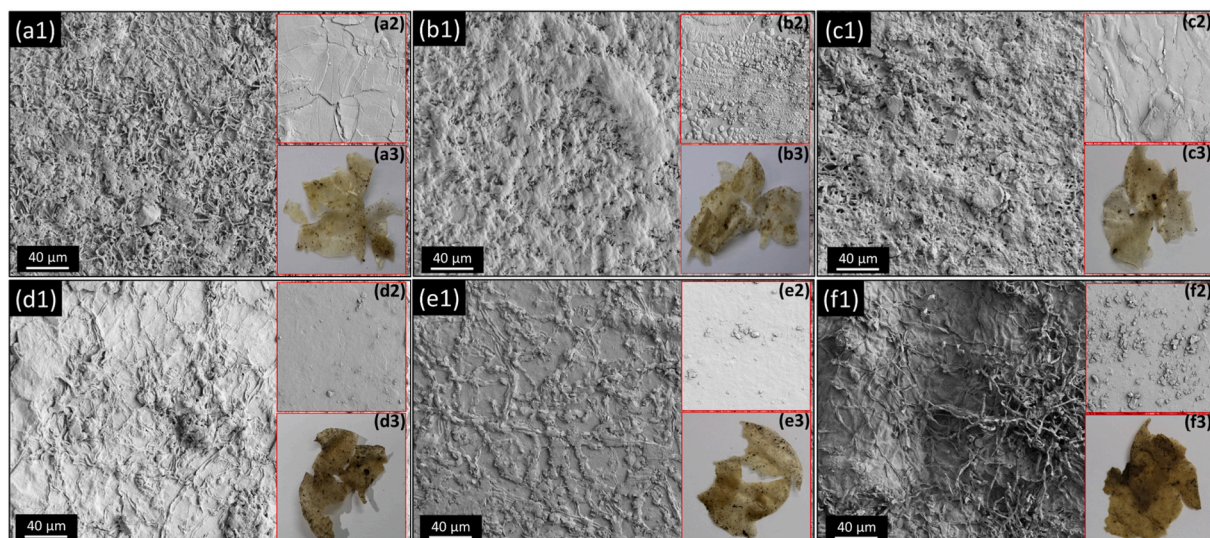


Fig. 4. SEM images showing the surface morphology of the films before and after the soil burial degradation test over four weeks. Furthermore, the digital photographs of the films post-degradation are presented: (a) CMC, (b) CMCC, (c) CMCC-NC5, (d) CMCC-NC10, (e) CMCC-NC20, and (f) CMCC-NC30.

the films appeared smooth and uniform, with minimal defects or irregularities, indicating a well-formed structure. This suggests good dispersion of clay and ChNFs within the CMC matrix, contributing to the film's initial integrity. After four weeks of soil burial degradation, noticeable changes in the surface morphology were observed. The surface became rougher, with visible cracks, pits, and signs of erosion. Additionally, some films exhibited a fibrous morphology, which was not present initially. This transition to a fibrous texture may be attributed to the degradation of the polymer matrix by soil microorganisms. As the biodegradable components of the films were broken down, the structure of the film became more porous, and the remaining fibrous network became more apparent. The observed fibrous morphology could result from the partial dissolution of the polymer matrix, exposing and concentrating the residual fibers. These observations indicate extensive microbial activity and degradation, aligning with the increased weight loss and changes in the film's physical properties noted in the degradation tests.

3.2.7. Assessment of antibacterial properties

The antimicrobial activity of the CMC-based films against *E. coli*, *S. aureus*, and *L. monocytogenes* is summarized in Table 4. No inhibition zones were observed for the CMC and CMCC control films against any of the tested bacteria. Similarly, the CMCC-NC5, CMCC-NC10, and CMCC-

NC20 films showed no antibacterial activity (Fig. S2). However, at the highest ChNF loading of 30%, the CMCC-NC30 film demonstrated significant antibacterial activity against all pathogens tested ($p < 0.05$), with inhibition zones ranging from 1.56 to 2.62 mm (Table 4 and Fig. 5). Notably, the strongest activity was observed against *E. coli*, a gram-negative bacterium. This group is particularly known for its higher resistance to antibiotic treatments, posing a significant public health challenge. Nevertheless, no significant differences in susceptibility were detected between the bacterial species ($p > 0.05$).

This effect is attributed to the interaction between the positively charged amino groups of chitin and the negatively charged bacterial cell membranes, leading to intracellular compound leakage and subsequent bacterial cell death (Helander et al., 2001). However, it is hypothesized that this mechanism is less effective against *S. aureus* due to its positively charged membrane, which may hinder the interaction and reduce antimicrobial activity. Ojagh et al. (Ojagh et al., 2010) observed that chitosan coatings containing cinnamon oil significantly inhibited bacterial growth in refrigerated rainbow trout. Similarly, Dehnad et al. (Dehnad et al., 2014) reported a 1 log CFU/g reduction in lactic acid bacteria in ground meat packaged with chitosan film compared to nylon packaging.

3.3. Environmental impact determination

The environmentally sustainable character of the developed films was verified through LCA (Chen et al., 2024). As a relevant and widely used indicator in the materials sector towards the SDGs agenda 2030 and achieving decarbonization goals (Backes & Traverso, 2022), the global warming potential (GWP) was first analyzed. The disaggregated values in Fig. 6a show that the neat CMC film had the lowest cradle-to-gate GWP with a value of 4.98 kg-CO₂ equiv.·kg⁻¹. Raw CMC acquisition, electricity consumption, and glycerin were the main contributors, with a share of 65.4, 13.6 and 11.2%, respectively. The incorporation of clay slightly increased the GWP to a maximum of 5.27 kg-CO₂ equiv.·kg⁻¹, mainly due to the sonication step that increases the energy consumption by 52.2%. Furthermore, the addition of ChNFs progressively reduced the GWP to reach a GWP of 5.07 kg-CO₂ equiv.·kg⁻¹ for the CMCC-NC30 counterpart. This decrease is due to the reduced impact of ChNFs when compared to the CMC polymer. To put these results in context, Fig. 6b provides a comparison with benchmark materials. In general, the GWP results of the developed films were comparable to industrially manufactured petroleum-derived polymers used in packaging

Table 4

Antibacterial activity of CMC, CMCC, and ChNF-containing films determined by agar diffusion assay.

Samples	<i>E. coli</i> ATCC 25922	<i>S. aureus</i> ATCC 29213	<i>L. monocytogenes</i> DSM 112142
	Zone of inhibition (in mm) ^a		
CMC	–	–	–
CMCC	–	–	–
CMCC-NC5	–	–	–
CMCC-NC10	–	–	–
CMCC-NC20	–	–	–
CMCC-NC30	2.62 ± 1.39 ^a	1.56 ± 0.54 ^a	2.09 ± 0.61 ^a
Cefaclor (30 μg)	16.00 ± 1.19 ^b	18.53 ± 0.76 ^b	16.90 ± 1.74 ^b

^a Averages (± standard deviation) were calculated from three experiments conducted in triplicate. Zones of inhibition (in mm) exclude the diameter of the disc. Different letters within the same bacterial group indicate significant differences between averages ($p < 0.05$). –: No zone of growth inhibition was observed.

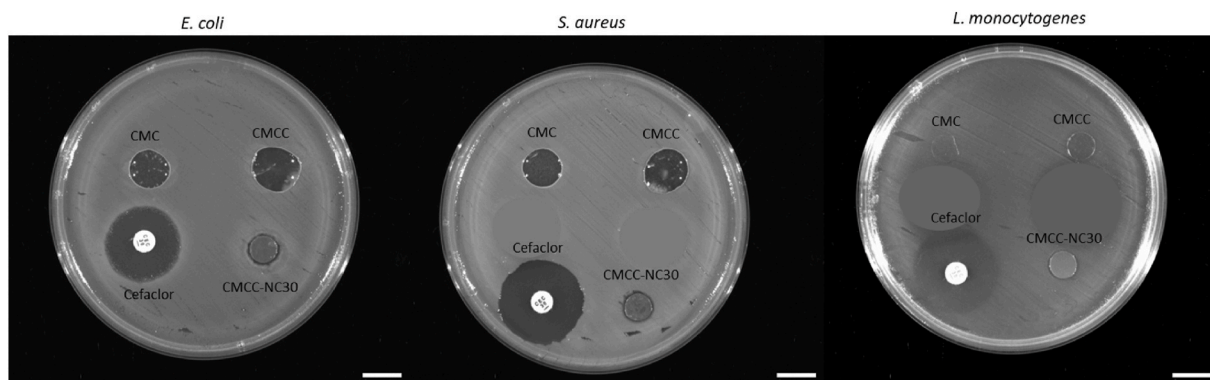


Fig. 5. Zones of inhibition formed by CMCC-NC30 against *E. coli*, *S. aureus*, and *L. monocytogenes*. CMC and CMCC films were used as negative controls. Cefaclor (30 μ g) was used as a positive control. Photos were taken using the ChemiDoc MP imaging system (Biorad) and are representative of one assay. The scale bar is 1 cm.

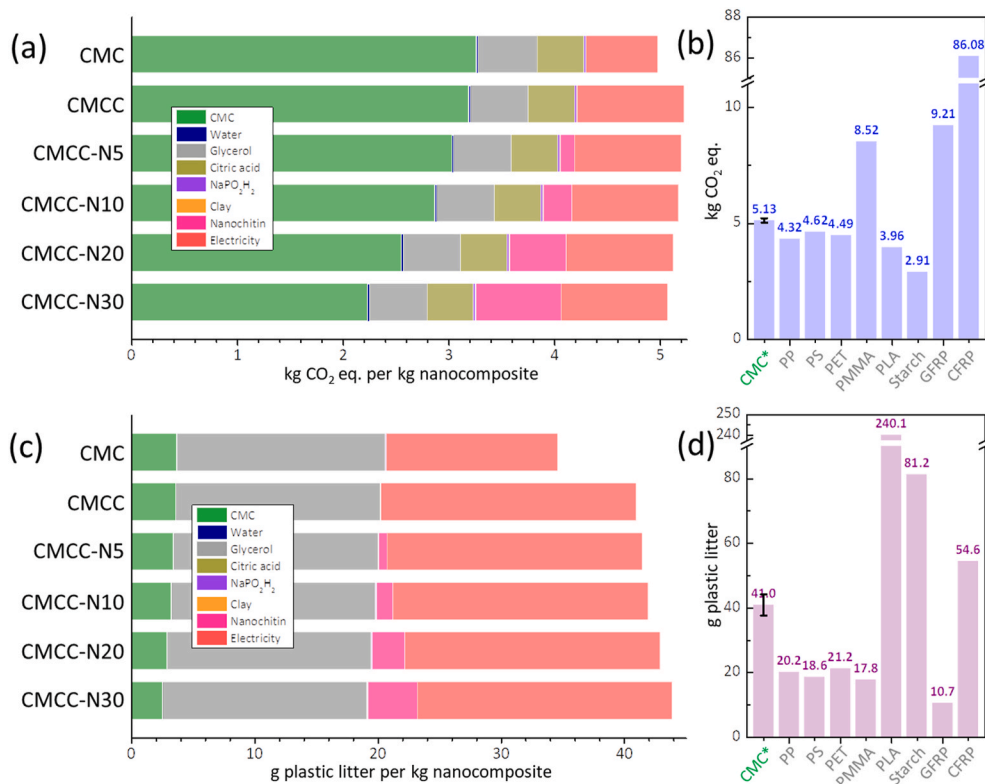


Fig. 6. Environmental impact of fabricated films: (a) disaggregated GWP per kilogram of film, (b) GWP comparison with benchmark materials, (c) disaggregated plastic litter generation per kilogram of film, and (d) plastic litter generation comparison with benchmark materials. CMC*: accounts for the mean and the standard deviation of all six nanocomposite films produced.

applications, and were slightly higher than the GWP of biobased polymers such as polylactide (PLA) or polyester-complexed starch (3.96 and 2.91 kg-CO₂ equiv.·kg⁻¹, respectively). It is also interesting to note that the developed antibacterial composite films had a significantly lower GWP when compared to carbon fibre reinforced plastic (CFRP) or glass fibre reinforced plastic (GFRP).

As a novel but relevant environmental impact metric, we used LCA to estimate the plastic litter over the life cycle of manufactured materials. Despite the multidimensional nature of LCA, plastic pollution has not been thoroughly analyzed so far (Julia Gutke, 2023). The main purpose is to shed further light and guide the implementation of materials that cause the least amount of plastic pollution. Such a calculation, which is a first rough estimate due to its low maturity, is obtained by estimating the plastic littering probability of all processes and multiplying it by the plastic content of all flows. The disaggregated plastic littering potential

along the supply chain in Fig. 6c shows values of 35–44 g of litter per kilogram of CMC and CMCC-NC30 processed, respectively. Glycerol and energy use emerge as the main contributors, with a combined share of 85–89%. As shown in Fig. 6d, these values remain well below the plastic littering estimated for biobased polymers such as PLA (240 g), polyester-complexed starch biopolymer (81 g), or CFRP (55 g). The higher plastic littering for biobased polymers is due to the plastic microcontainers of fertilizers and pesticides that become litter at a very high rate. Overall, Fig. 6 shows a good balance of carbon footprint and plastic littering for CMC/nanoclay/nanochitin films compared to the benchmark materials.

Considering additional impact categories can help to understand the trade-offs of the materials. As disclosed in Fig. 7, the *terrestrial acidification*, *particulate matter formation*, and *photochemical oxidant formation* categories show a similar trend. Here, the impact of CMC

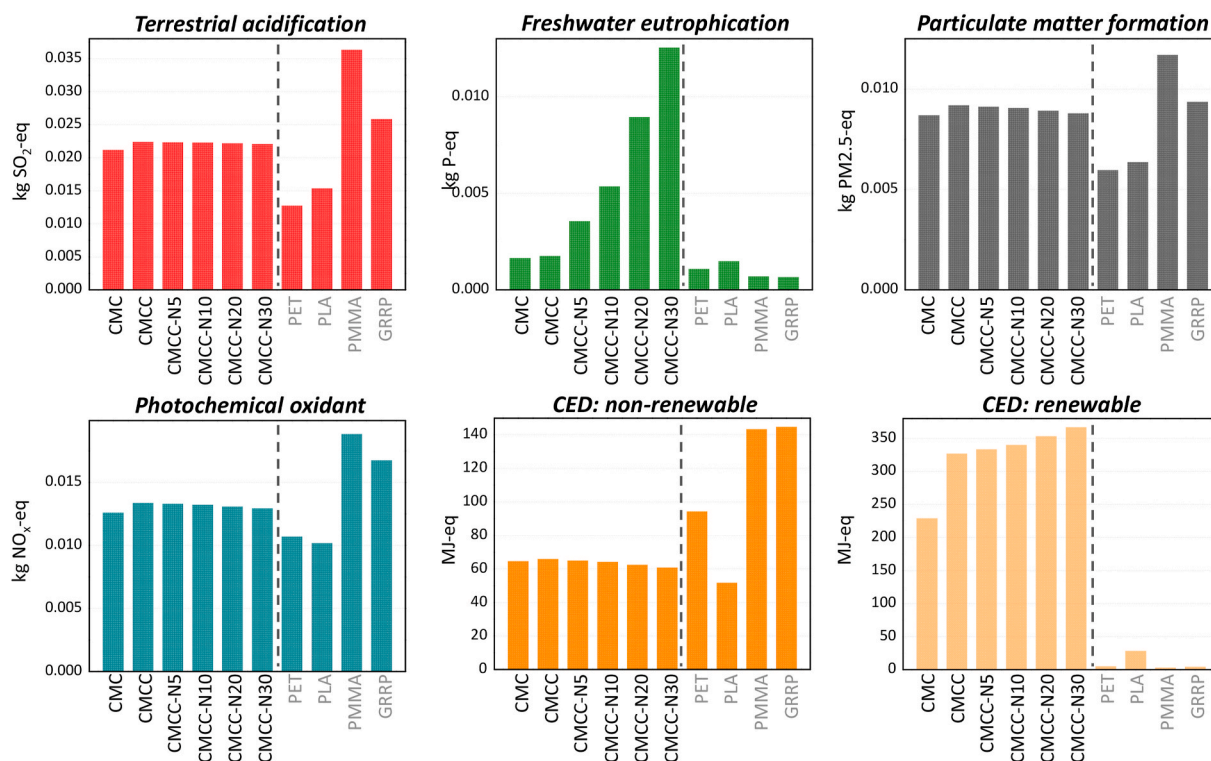


Fig. 7. Environmental impacts of CMC/nanoclay/nanochitin nanocomposite films and its competitors normalized to 1 kg of material.

nanocomposites remains slightly higher than that of conventional packaging materials such as polyethylene terephthalate (PET) and (PLA), but lower than that of poly(methyl methacrylate) (PMMA) or GFRP. However, the materials developed here score very high in *freshwater eutrophication*, mainly due to the wastewater treatment required during nanochitin production from fungi. In addition, the large share of renewable resources (biobased materials, renewable energy grid) results in low *non-renewable CED* values compared to those observed for the benchmark materials. Nevertheless, the *renewable CED* values, which increase for the nanocomposites composed of nanoclay and nanochitin, are notably high (293–427 vs. 3–28 MJ equiv.). Such large values originate from the laboratory-scale production of the materials, which requires 51–76 kWh per kilogram of processed film. Therefore, further upscaling and implementation of energy-saving processing can substantially reduce the overall impact of CMC-based nanocomposite films (Piccinno et al., 2018).

3.4. Integrated analysis of the CMC-based film properties for food packaging applications

The performance of CMC-based films in food packaging applications is driven by the interplay between their permeability, mechanical properties, surface wettability, and biodegradability. Understanding the relationships between these properties is crucial for optimizing the functionality of the films.

Mechanical properties and permeability. A clear correlation exists between the mechanical properties and permeability of the films. The addition of 3% (w/w) clay significantly enhanced tensile strength and modulus, creating a denser, more compact matrix that also reduced ORT and WVP. This improved mechanical integrity contributes to the formation of a robust barrier, effectively limiting gas and moisture diffusion. Similarly, increasing ChNF content further reduced permeability while enhancing the mechanical properties. However, the observed decline in mechanical performance at low and very high nanochitin concentrations—due to particle dispersion and agglomeration issues—highlights the importance of achieving uniform filler

distribution to optimize both reinforcement and barrier properties.

Wettability and permeability. Surface wettability, as indicated by contact angle measurements, plays a critical role in the films' interaction with moisture and their permeability. Films with higher wettability (lower contact angles) tend to absorb more moisture, leading to increased permeability. For example, the pure CMC film, with a contact angle of 34°, exhibited moderate permeability to oxygen and water vapor. The introduction of clay raised the contact angle to 52°, indicating enhanced hydrophobicity, which was accompanied by a notable reduction in permeability. This suggests that the increased hydrophobicity, driven by the denser matrix structure, improved the film's barrier performance. ChNF addition increased the contact angle, indicating reduced wettability and further improved barrier properties.

Wettability and biodegradability. The relationship between surface wettability and biodegradability is equally important, as wettability influences the film's interaction with moisture in the environment. Hydrophilic surfaces with lower contact angles typically degrade faster due to greater moisture absorption and increased microbial activity. The pure CMC film, with its contact angle of 34°, demonstrated a high degradation rate of 50.5% over four weeks. In contrast, incorporating 3% clay into the CMC matrix increased the hydrophobicity, slowing the degradation rate to 37.3%. ChNF addition showed a complex effect: at lower concentrations (5%), increased hydrophilicity accelerated degradation (40.8% weight loss at four weeks). However, at higher concentrations, the contact angle rose again, slowing the degradation rate slightly due to the formation of a more hydrophobic surface, although biodegradation remained significant at 52.1% by the fourth week.

Sustainability and antimicrobial functionality. The incorporation of ChNF into CMC-based films significantly enhanced both their antimicrobial functionality and environmental sustainability. At higher concentrations, particularly 30%, ChNFs imparted antibacterial properties against *E. coli*, *S. aureus*, and *L. monocytogenes*, due to their large surface area and active functional groups that disrupt bacterial membranes. This antimicrobial effect not only improves food safety by reducing contamination risks but also complements the films' overall barrier

performance. From an environmental perspective, the biogenic and renewable nature of nanochitin, together with its minimal top-down processing, contributes to a reduced carbon footprint, as confirmed by LCA. Films containing ChNFs exhibited lower GWP and potentially generated less plastic waste along their supply chain compared to petroleum-based alternatives. The renewable sourcing of ChNFs, derived from fungal biomass, and its minimal reliance on fossil fuels further reduced environmental impact. This combination of antimicrobial effectiveness and environmental benefits makes ChNFs-enhanced CMC films an ideal solution for sustainable food packaging, offering both improved protection against pathogens and alignment with global sustainability goals.

This analysis demonstrates the strong interconnection between permeability, mechanical properties, wettability, and biodegradability in CMC-based composite films. The synergistic effects of clay and ChNFs enhance the statifilms' barrier properties, mechanical strength, and biodegradability, making these materials promising candidates for sustainable food packaging solutions. Furthermore, the incorporation of ChNFs significantly improves antimicrobial functionality, offering enhanced protection against pathogens, and contributes to environmental sustainability by reducing carbon footprint and plastic waste. By carefully balancing hydrophilic and hydrophobic components, optimizing filler distribution, and leveraging the antibacterial and environmental benefits of ChNFs, these films present a compelling solution that meets both functional and ecological requirements in modern food packaging.

4. Conclusions

This study develops and characterizes sustainable and eco-friendly CMC-based composite films for food packaging applications, incorporating ChNFs and clay. The films demonstrate enhanced mechanical strength, moisture resistance, gas barrier properties, biodegradability, and antibacterial activity, making them a promising alternative to conventional packaging materials derived from fossil sources. The following key findings highlight the novel contributions of this work.

- The addition of 3% clay improved tensile strength (by 90%) and modulus (by 445%) and reduced OTR and WVP, enhancing the films' suitability for food packaging applications.
- Incorporating ChNFs further improved the films' barrier performance and biodegradability, with a 52.1% weight loss after four weeks of soil burial, demonstrating the films' potential for sustainable disposal.
- Films with the highest ChNF content (30%) exhibited antibacterial activity against *E. coli*, *S. aureus*, and *L. monocytogenes*.
- The LCA results showed a GWP of 5.0–5.3 kg CO₂-equiv./kg, comparable to biobased and petroleum-based polymers with well-optimized supply chains, and identified CMC acquisition (44–65%) and electricity consumption (13–20%) as the main environmental hotspots.
- The films potentially yielded 35–44 g of plastic litter per kg along their supply chain, which is lower than competing bio-based materials or high-performance composites, highlighting their environmental attributes.

Overall, this study confirms that the integration of fungal-derived ChNFs improved functional performance while offering an environmentally sustainable alternative, showcasing the value of biobased composites in reducing environmental impact. With enhanced mechanical strength, barrier performance, biodegradability, and antimicrobial properties, these films presented a promising alternative to conventional plastic packaging, addressing the growing demand for eco-friendly solutions.

CRedit authorship contribution statement

Hossein Baniasadi: Writing – review & editing, Writing – original draft, Visualization, Validation, Supervision, Project administration, Methodology, Investigation, Formal analysis, Conceptualization. **Ziba Fathi:** Writing – review & editing, Methodology, Investigation, Formal analysis. **Cristina D. Cruz:** Writing – review & editing, Writing – original draft, Validation, Methodology, Investigation, Formal analysis, Conceptualization. **Roozbeh Abidnejad:** Writing – review & editing, Methodology, Formal analysis. **Päivi Tammela:** Writing – review & editing, Funding acquisition. **Jukka Niskanen:** Writing – review & editing, Funding acquisition. **Erlantz Lizundia:** Writing – review & editing, Writing – original draft, Supervision, Methodology, Investigation, Funding acquisition, Formal analysis, Conceptualization.

Declaration of competing interest

The authors declare that they have no known competing financial interests or personal relationships that could have appeared to influence the work reported in this paper.

Acknowledgment

The authors would like to acknowledge the funding of the Research Council of Finland, No. 327248 (ValueBiomat). The authors acknowledge financial support from the University of the Basque Country (Convocatoria de ayudas a grupos de investigación GIU21/010). The DDCB unit at the Faculty of Pharmacy, supported by HiLIFE and Bio-center Finland, is gratefully acknowledged for providing access to microbiology facilities and instruments. R.A. acknowledges funding from Business Finland Strategic Centres for Science, Technology, and Innovation IMD1/Kontturi. This work made use of Aalto University Bioeconomy Facilities and OtaNano, Nanomicroscopy Center (Aalto-NMC).

Appendix A. Supplementary data

Supplementary data to this article can be found online at <https://doi.org/10.1016/j.foodhyd.2024.110987>.

Data availability

Data will be made available on request.

References

- Afshar, S., & Baniasadi, H. (2018). Investigation the effect of graphene oxide and gelatin/starch weight ratio on the properties of starch/gelatin/GO nanocomposite films: The RSM study. *International Journal of Biological Macromolecules*, 109. <https://doi.org/10.1016/j.ijbiomac.2017.11.083>
- Alkassfariy, A. N., Yassin, M. A., Abdel Rehim, M. H., Liu, L., Jiao, Z., Wang, B., & Wei, Z. (2024). Modified cellulose nanocrystals enhanced polycaprolactone multifunctional films with barrier, UV-blocking and antimicrobial properties for food packaging. *International Journal of Biological Macromolecules*, 261, Article 129871. <https://doi.org/10.1016/j.ijbiomac.2024.129871>
- Alshehri, A. A., Hamed, Y. S., Kamel, R. M., Shawir, S. M. S., Sakr, H., Ali, M., Ammar, A., Saleh, M. N., El Fadly, E., Salama, M. A., & Abdin, M. (2024). Enhanced physical properties, antioxidant and antibacterial activity of bio-composite films composed from carboxymethyl cellulose and polyvinyl alcohol incorporated with broccoli sprout seed extract for butter packaging. *International Journal of Biological Macromolecules*, 255, Article 128346. <https://doi.org/10.1016/j.ijbiomac.2023.128346>
- Azpirtarte Aretxabaleta, M., Barandika, G., Minguez, R., & Lizundia, E. (2024). Fungal chitin nanofibrils improve mechanical performance and UV-light resistance in carboxymethylcellulose and polyvinylpyrrolidone films. *Biomacromolecules*. <https://doi.org/10.1021/acs.biomac.4c00846>
- Backes, J. G., & Traverso, M. (2022). Life cycle sustainability assessment as a metrics towards SDGs agenda 2030. *Current Opinion in Green and Sustainable Chemistry*, 38, Article 100683. <https://doi.org/10.1016/j.cogsc.2022.100683>
- Baharlouei, P., & Rahman, A. (2022). Chitin and chitosan: Prospective biomedical applications in drug delivery, cancer treatment, and wound healing. *Marine Drugs*, 20(7), 460. <https://doi.org/10.3390/md20070460>

- Bangar, S., Ilyas, R. A., Chowdhury, A., Navaf, M., Sunooj, K. V., & Siroha, A. K. (2023). Bentonite clay as a nanofiller for food packaging applications. *Trends in Food Science & Technology*, 142, Article 104242. <https://doi.org/10.1016/j.tifs.2023.104242>
- Baniasadi, H., Fathi, Z., Lizundia, E., Cruz, C. D., Abidnejad, R., Fazeli, M., Tammela, P., Kontturi, E., Lipponen, J., & Niskanen, J. (2024). Development and characterization of pomegranate peel extract-infused carboxymethyl cellulose composite films for functional, sustainable food packaging. *Food Hydrocolloids*, 158, Article 110525. <https://doi.org/10.1016/j.foodhyd.2024.110525>
- Baniasadi, H., Trifol, J., Lipponen, S., & Seppälä, J. (2021). Sustainable composites of surface-modified cellulose with low-melting point polyamide. *Materials Today Chemistry*, 22, Article 100590. <https://doi.org/10.1016/j.mtchem.2021.100590>
- Basbasan, A. J., Hararak, B., Winotapun, C., Wanmolee, W., Leelaphiwat, P., Boonruang, K., Chinsirikul, W., & Chonhenchob, V. (2022). Emerging challenges on viability and commercialization of lignin in biobased polymers for food packaging: A review. *Food Packaging and Shelf Life*, 34, Article 100969. <https://doi.org/10.1016/j.fpsl.2022.100969>
- Brito, R. S. de, Costa, M. J. A., Barbosa, J. R., Filho, A. F. S., de Souza Farias, F., & Lourenço, L. de F. H. (2023). K-Nearest Neighbor algorithm for selection of new gelatin-carboxymethylcellulose films with TiO₂ nanoparticles and propolis extract with antioxidant and light barrier activity. *Food Packaging and Shelf Life*, 38, Article 101119. <https://doi.org/10.1016/j.fpsl.2023.101119>
- Chen, L., Bi, T., Lizundia, E., Liu, A., Qi, L., Ma, Y., Huang, J., Lu, Z., Yu, L., Deng, H., & Chen, C. (2024). Biomass waste-assisted micro(nano)plastics capture-utilization-storage (PCUS) for sustainable water remediation. *Innovation*. <https://doi.org/10.1016/j.xinn.2024.100655>
- CLSI M02-A12, CLSI M100-S26. <https://webstore.ansi.org/standards/cls/clsim02a12m100s26>
- Coles, R., McDowell, D., & Kirwan, M. J. (2003). *Food packaging technology* (Vol. 5). CRC press.
- Dairi, N., Ferfera-Harrar, H., Ramos, M., & Garrigós, M. C. (2019). Cellulose acetate/AgNPs-organoclay and/or thymol nano-biocomposite films with combined antimicrobial/antioxidant properties for active food packaging use. *International Journal of Biological Macromolecules*, 121, 508–523. <https://doi.org/10.1016/j.ijbiomac.2018.10.042>
- Dehnad, D., Mirzaei, H., Emam-Djomeh, Z., Jafari, S.-M., & Dadashi, S. (2014). Thermal and antimicrobial properties of chitosan-nanocellulose films for extending shelf life of ground meat. *Carbohydrate Polymers*, 109, 148–154. <https://doi.org/10.1016/j.carbpol.2014.03.063>
- Dong, X., Shang, J., Xiao, T., Song, R., Sheng, X., Li, N., Zhang, J., & Ping, Q. (2024). A facile method to fabricate sustainable bamboo ethanol lignin/carboxymethylcellulose films with efficient anti-ultraviolet and insulation properties. *International Journal of Biological Macromolecules*, 273, Article 132959. <https://doi.org/10.1016/j.ijbiomac.2024.132959>
- Duarte, M. L., Ferreira, M. C., Marvão, M. R., & Rocha, J. (2002). An optimised method to determine the degree of acetylation of chitin and chitosan by FTIR spectroscopy. *International Journal of Biological Macromolecules*, 31(1), 1–8. [https://doi.org/10.1016/S0141-8130\(02\)00039-9](https://doi.org/10.1016/S0141-8130(02)00039-9)
- El Mouzahim, M., Eddarai, E. M., Eladaoui, S., Guenbour, A., Bellaouchou, A., Zarrouk, A., & Boussen, R. (2023a). Food packaging composite film based on chitosan, natural kaolinite clay, and Ficus. carica leaves extract for fresh-cut apple slices preservation. *International Journal of Biological Macromolecules*, 233, Article 123430. <https://doi.org/10.1016/j.ijbiomac.2023.123430>
- El Mouzahim, M., Eddarai, E. M., Eladaoui, S., Guenbour, A., Bellaouchou, A., Zarrouk, A., & Boussen, R. (2023b). Effect of Kaolin clay and Ficus carica mediated silver nanoparticles on chitosan food packaging film for fresh apple slice preservation. *Food Chemistry*, 410, Article 135470. <https://doi.org/10.1016/j.foodchem.2023.135470>
- Espartero, A., Bello Álvarez, C., & Lizundia Fernández, E. (2023). Cytotoxicity and inflammatory effects of chitin nanofibrils isolated from fungi. *Biological Macromolecules*, 24(12), 5737–5748. <https://doi.org/10.1021/acs.biomac.3c00710>
- Fernández-Santos, J., Valls, C., Cusola, O., & Roncero, M. B. (2022). Composites of cellulose nanocrystals in combination with either cellulose nanofibril or carboxymethylcellulose as functional packaging films. *International Journal of Biological Macromolecules*, 211, 218–229. <https://doi.org/10.1016/j.ijbiomac.2022.05.049>
- Fiori, A. P. S., Camani, P. H., dos Santos Rosa, D., & Carastan, D. J. (2019). Combined effects of clay minerals and polyethylene glycol in the mechanical and water barrier properties of carboxymethylcellulose films. *Industrial Crops and Products*, 140, Article 111644. <https://doi.org/10.1016/j.indcrop.2019.111644>
- Ganjeh, A. M., Saraiva, J. A., Pinto, C. A., Casal, S., & Gonçalves, I. (2024). Recent advances in nano-reinforced food packaging based on biodegradable polymers using layer-by-layer assembly: A review. *Carbohydrate Polymer Technologies and Applications*, 7, Article 100395. <https://doi.org/10.1016/j.carpta.2023.100395>
- Gasti, T., & Dixit, S. (2024). Development of poly (vinyl alcohol)/nano-calcium/Ipomoea carica anthocyanin based halochromic smart films for freshness monitoring of lamb meat. *Food Bioscience*, 60, Article 104441. <https://doi.org/10.1016/j.fbio.2024.104441>
- Greca, L. G., Azpiazu, A., Reyes, G., Rojas, O. J., Tardy, B. L., & Lizundia, E. (2024). Chitin-based pulps: Structure-property relationships and environmental sustainability. *Carbohydrate Polymers*, 325, Article 121561. <https://doi.org/10.1016/j.carbpol.2023.121561>
- Gülpınar, M., Tomul, F., Arslan, Y., & Tran, H. N. (2024). Chitosan-based film incorporated with silver-loaded organo-bentonite or organo-bentonite: Synthesis and characterization for potential food packaging material. *International Journal of Biological Macromolecules*, 274, Article 133197. <https://doi.org/10.1016/j.ijbiomac.2024.133197>
- Halloub, A., Nekhlouai, S., Raji, M., Essabir, H., Bensalah, M., Bouhfid, R., & Qaiss, A. (2024). UV-Activated self-healing food packaging: ω-3 based microcapsules in hemicellulose/chitosan blend film for cashew nut preservation. *Food Bioscience*, 60, Article 104313. <https://doi.org/10.1016/j.fbio.2024.104313>
- Helander, I. M., Nurmiaho-Lassila, E.-L., Ahvenainen, R., Rhoades, J., & Roller, S. (2001). Chitosan disrupts the barrier properties of the outer membrane of Gram-negative bacteria. *International Journal of Food Microbiology*, 71(2), 235–244. [https://doi.org/10.1016/S0168-1605\(01\)00609-2](https://doi.org/10.1016/S0168-1605(01)00609-2)
- Heux, L., Brugnerotto, J., Desbrières, J., Versali, M.-F., & Rinaudo, M. (2000). Solid state NMR for determination of degree of acetylation of chitin and chitosan. *Biomacromolecules*, 1(4), 746–751. <https://doi.org/10.1021/bm000070y>
- Heydarian, A., & Shavisi, N. (2023). Multifunctional food packaging materials: Electrospun mats based on gelatin-xanthan gum containing chitin nanofibers and black barberry anthocyanins for freshness monitoring and enhancing the shelf-life quality of Pacific white shrimps. *Food Packaging and Shelf Life*, 40, Article 101219. <https://doi.org/10.1016/j.fpsl.2023.101219>
- Hou, T., Sana, S. S., Riah, Z., Kim, J. T., Bharathi, A., Kim, S.-C., & Roy, S. (2024). Fabrication of nanoceria and metakaolin activated poly (butylene adipate-co-terephthalate)-based composite for active food packaging applications. *Food Bioscience*, 61, Article 104900. <https://doi.org/10.1016/j.fbio.2024.104900>
- Jahangiri, F., Mohanty, A. K., & Misra, M. (2024). Sustainable biodegradable coatings for food packaging: Challenges and opportunities. *Green Chemistry*, 26(9), 4934–4974. <https://doi.org/10.1039/d3gc02647g>
- Julia Gutke, A. C. (2023). *Plex – plastic litter Extension for ecoinvent*.
- Jurić, M., Maslov Bandić, L., Carullo, D., & Jurić, S. (2024). Technological advancements in edible coatings: Emerging trends and applications in sustainable food preservation. *Food Bioscience*, 58, Article 103835. <https://doi.org/10.1016/j.fbio.2024.103835>
- Kasaai, M. R. (2010). Determination of the degree of N-acetylation for chitin and chitosan by various NMR spectroscopy techniques: A review. *Carbohydrate Polymers*, 79(4), 801–810. <https://doi.org/10.1016/j.carbpol.2009.10.051>
- Kaur, M. M., Sharma, S., Kalia, A., & Jawandha, S. K. (2024). Maize starch-PVA nanocomposite biodegradable antimicrobial packaging films for enhancement of shelf-life of *Agaricus bisporus*. *Sustainable Materials and Technologies*, Article e01114. <https://doi.org/10.1016/j.susmat.2024.e01114>
- Khazaei, F., Shavisi, N., & Shahbazi, Y. (2024). Intelligent pH-sensitive tragacanth gum-pectin nanofiber mats encapsulating *Althaea officinalis* extract and chitin nanowhiskers to track the freshness of chicken filets. *Lebensmittel-Wissenschaft & Technologie*, 206, Article 116606. <https://doi.org/10.1016/j.lwt.2024.116606>
- Khezrian, A., & Shahbazi, Y. (2018). Application of nanocomposite chitosan and carboxymethyl cellulose films containing natural preservative compounds in minced camel's meat. *International Journal of Biological Macromolecules*, 106, 1146–1158. <https://doi.org/10.1016/j.ijbiomac.2017.08.117>
- Kim, J.-K., Oh, S. H., Song, M.-O., Jang, S., Kang, S. J., Kwak, S. K., & Jin, J. (2024). Wholly bio-based, ultra-tough, transparent PLA composites reinforced with nanocellulose and nanochitin. *Composites Part B: Engineering*, 281, Article 111563. <https://doi.org/10.1016/j.compositesb.2024.111563>
- Kramar, A., González-Benito, J., Nikolić, N., Larranaga, A., & Lizundia, E. (2024). Properties and environmental sustainability of fungal chitin nanofibril reinforced cellulose acetate films and nanofiber mats by solution blow spinning. *International Journal of Biological Macromolecules*, 269, Article 132046. <https://doi.org/10.1016/j.ijbiomac.2024.132046>
- Laurent, A., Weidema, B. P., Bare, J., Liao, X., Maia de Souza, D., Pizzolo, M., Sala, S., Schreiber, H., Thonemann, N., & Verones, F. (2020). Methodological review and detailed guidance for the life cycle interpretation phase. *Journal of Industrial Ecology*, 24(5), 986–1003. <https://doi.org/10.1111/jiec.13012>
- Li, M.-C., Wu, Q., Song, K., Cheng, H. N., Suzuki, S., & Lei, T. (2016). Chitin nanofibers as reinforcing and antimicrobial agents in carboxymethyl cellulose films: Influence of partial deacetylation. *ACS Sustainable Chemistry & Engineering*, 4(8), 4385–4395. <https://doi.org/10.1021/acsuscchemeng.6b00981>
- Li, W., Zhang, J., Chen, X., Zhou, X., Zhou, J., Sun, H., Wang, S., & Liu, Y. (2024). Organic nanoparticles incorporated starch/carboxymethylcellulose multifunctional coating film for efficient preservation of perishable products. *International Journal of Biological Macromolecules*, 275, Article 133357. <https://doi.org/10.1016/j.ijbiomac.2024.133357>
- Liu, X., Qin, Z., Ma, Y., Liu, H., & Wang, X. (2023). Cellulose-based films for food packaging applications: Review of preparation, properties, and prospects. *Journal of Renewable Materials*, 11(8), 3203–3225. <https://doi.org/10.32604/jrm.2023.027613>
- Majumder, S., Huang, S., Zhou, J., Wang, Y., & George, S. (2023). Tannic acid-loaded halloysite clay grafted with silver nanoparticles enhanced the mechanical and antimicrobial properties of soy protein isolate films for food-packaging applications. *Food Packaging and Shelf Life*, 39, Article 101142. <https://doi.org/10.1016/j.fpsl.2023.101142>
- Mao, L., Zuo, J., Liu, Y., Zheng, B., Dai, X., Bai, Z., Liu, Y., & Yao, J. (2023). Alginate based films integrated with nitrogen-functionalized carbon dots and layered clay for active food packaging applications. *International Journal of Biological Macromolecules*, 253, Article 126653. <https://doi.org/10.1016/j.ijbiomac.2023.126653>
- Mishra, B., Panda, J., Mishra, A. K., Nath, P. C., Nayak, P. K., Mahapatra, U., Sharma, M., Chopra, H., Mohanta, Y. K., & Sridhar, K. (2024). Recent advances in sustainable biopolymer-based nanocomposites for smart food packaging: A review. *International Journal of Biological Macromolecules*, 135583. <https://doi.org/10.1016/j.ijbiomac.2024.135583>
- Mohammadpour Velni, S., Baniasadi, H., & Vaziri, A. (2018). Fabrication and characterization of antimicrobial starch-based nanocomposite films and modeling the process parameters via the RSM. *Polymer Composites*, 39. <https://doi.org/10.1002/pc.24733>

- Mohsen, A. H., Ali, N. A., Hussein, S. I., Mohammed, A. Y. A., Alraih, A. M., & Abd-Elnaiem, A. M. (2024). Investigation of optical, mechanical, thermal, wettability, and antibacterial activity of polyvinyl alcohol mixed with clay nanoparticles. *Inorganic Chemistry Communications*, 167, Article 112841. <https://doi.org/10.1016/j.inoche.2024.112841>
- Molina-Besch, K., & Keszleri, H. (2023). Exploring the industrial perspective on biobased plastics in food packaging applications – insights from Sweden. *Sustainable Production and Consumption*, 35, 72–84. <https://doi.org/10.1016/j.spc.2022.10.018>
- Motloung, M. P., Mofokeng, T. G., Bandyopadhyay, J., & Ray, S. S. (2024). Properties and soil degradation characteristics of chitin-reinforced poly (butylene succinate)/hydroxyapatite composites. *Macromolecular Materials and Engineering*, 309(8), Article 2300293. <https://doi.org/10.1002/mame.202300293>
- Nawawi, W. M., Lee, K.-Y., Kontturi, E., Murphy, R. J., & Bismarck, A. (2019). Chitin nanopaper from mushroom extract: Natural composite of nanofibers and glucan from a single biobased source. *ACS Sustainable Chemistry & Engineering*, 7(7), 6492–6496. <https://doi.org/10.1021/acssuschemeng.9b00721>
- Ngasotter, S., Xavier, K. A. M., Meitei, M. M., Waikhom, D., Madhulika, Pathak, J., & Singh, S. K. (2023). Crustacean shell waste derived chitin and chitin nanomaterials for application in agriculture, food, and health – a review. *Carbohydrate Polymer Technologies and Applications*, 6, Article 100349. <https://doi.org/10.1016/j.carpta.2023.100349>
- Ojagh, S. M., Rezaei, M., Razavi, S. H., & Hosseini, S. M. H. (2010). Effect of chitosan coatings enriched with cinnamon oil on the quality of refrigerated rainbow trout. *Food Chemistry*, 120(1), 193–198. <https://doi.org/10.1016/j.foodchem.2009.10.006>
- Oun, A. A., & Rhim, J.-W. (2017a). Effect of oxidized chitin nanocrystals isolated by ammonium persulfate method on the properties of carboxymethyl cellulose-based films. *Carbohydrate Polymers*, 175, 712–720. <https://doi.org/10.1016/j.carbpol.2017.08.052>
- Oun, A. A., & Rhim, J.-W. (2017b). Preparation of multifunctional chitin nanowhiskers/ZnO-Ag NPs and their effect on the properties of carboxymethyl cellulose-based nanocomposite film. *Carbohydrate Polymers*, 169, 467–479. <https://doi.org/10.1016/j.carbpol.2017.04.042>
- Oun, A. A., & Rhim, J.-W. (2020). Preparation of multifunctional carboxymethyl cellulose-based films incorporated with chitin nanocrystal and grapefruit seed extract. *International Journal of Biological Macromolecules*, 152, 1038–1046. <https://doi.org/10.1016/j.ijbiomac.2019.10.191>
- Piccino, F., Hischer, R., Seeger, S., & Som, C. (2018). Predicting the environmental impact of a future nanocellulose production at industrial scale: Application of the life cycle assessment scale-up framework. *Journal of Cleaner Production*, 174, 283–295. <https://doi.org/10.1016/j.jclepro.2017.10.226>
- Priyadarshi, R., Kim, S.-M., & Rhim, J.-W. (2021). Carboxymethyl cellulose-based multifunctional film combined with zinc oxide nanoparticles and grape seed extract for the preservation of high-fat meat products. *Sustainable Materials and Technologies*, 29, Article e00325. <https://doi.org/10.1016/j.susmat.2021.e00325>
- Priyadarshi, R., Roy, S., Ghosh, T., Biswas, D., & Rhim, J.-W. (2022). Antimicrobial nanofillers reinforced biopolymer composite films for active food packaging applications - a review. *Sustainable Materials and Technologies*, 32, Article e00353. <https://doi.org/10.1016/j.susmat.2021.e00353>
- Rabea, E. I., Badawy, M. E.-T., Stevens, C. V., Smaghe, G., & Steurbaut, W. (2003). Chitosan as antimicrobial agent: Applications and mode of action. *Biomacromolecules*, 4(6), 1457–1465. <https://doi.org/10.1021/bm034130m>
- Ramakrishnan, R., Kim, J. T., Roy, S., & Jayakumar, A. (2024). Recent advances in carboxymethyl cellulose-based active and intelligent packaging materials: A comprehensive review. *International Journal of Biological Macromolecules*, 259, Article 129194. <https://doi.org/10.1016/j.ijbiomac.2023.129194>
- Rathee, S., Singh, K. R. B., Mallick, S., Singh, J., Pandey, S. S., Ojha, A., & Singh, R. P. (2024). Smart alginate nanomaterials: Revolutionizing food across delivery, preservation, packaging, safety, and waste upcycling. *Carbohydrate Polymer Technologies and Applications*, 100568. <https://doi.org/10.1016/j.carpta.2024.100568>
- Ren, H., Huang, Y., Yang, W., Ling, Z., Liu, S., Zheng, S., Li, S., Wang, Y., Pan, L., Fan, W., & Zheng, Y. (2024). Emerging nanocellulose from agricultural waste: Recent advances in preparation and applications in biobased food packaging. *International Journal of Biological Macromolecules*, 277, Article 134512. <https://doi.org/10.1016/j.ijbiomac.2024.134512>
- Rezaei, F., Tajik, H., & Shahbazi, Y. (2023). Intelligent double-layer polymers based on carboxymethyl cellulose-cellulose nanocrystals film and poly(lactic acid)-Viola odorata petal anthocyanins nanofibers to monitor food freshness. *International Journal of Biological Macromolecules*, 252, Article 126512. <https://doi.org/10.1016/j.ijbiomac.2023.126512>
- Robertson, G. L. (2009). *Food packaging and shelf life: A practical guide*. CRC Press.
- Ruiz, D., Veronica, F. M., & Markus Niederberger, E. L. (2023). Chitin nanofibrils from fungi for hierarchical gel polymer electrolytes enabling transient zinc ion batteries with stable Zn electrodeposition. *Small*, 19(45), Article 2303394. <https://doi.org/10.1002/sml.202303394>
- Sagaya Deva Niranjana, X., & Krishnamoorthy, R. (2024). Chitin extraction from *Lutjanus campechanus* for sustainable bio-plastic production (red snapper). *Biomedical Materials & Devices*, 1–12. <https://doi.org/10.1007/s44174-024-00181-5>
- Shan, Z., Huang, J., Huang, Y., Zhou, Y., & Li, Y. (2024a). Carboxymethylcellulose and rare earth metal cation self-assembly: Tunable encapsulation of carbon dots in a multifunctional transparent film. *Chemical Engineering Journal*, 496, Article 154275. <https://doi.org/10.1016/j.cej.2024.154275>
- Shan, Z., Huang, J., Huang, Y., Zhou, Y., & Li, Y. (2024b). Copper ions reinforced flexible carboxymethylcellulose/polyethyleneimine composite films with enhanced mechanical properties, UV-shielding performance, thermal stability, solvent resistance, and antibacterial activity. *International Journal of Biological Macromolecules*, 259, Article 129281. <https://doi.org/10.1016/j.ijbiomac.2024.129281>
- Subramani, G., & Manian, R. (2024). Bioactive chitosan films: Integrating antibacterial, antioxidant, and antifungal properties in food packaging. *International Journal of Biological Macromolecules*, 278, Article 134596. <https://doi.org/10.1016/j.ijbiomac.2024.134596>
- Sun, F., Shan, P., Liu, B., Li, Y., Wang, K., Zhuang, Y., Ning, D., & Li, H. (2024). Gelatin-based multifunctional composite films integrated with dialdehyde carboxymethyl cellulose and coffee leaf extract for active food packaging. *International Journal of Biological Macromolecules*, 263, Article 130302. <https://doi.org/10.1016/j.ijbiomac.2024.130302>
- Tamina, S. K., & Rhim, J.-W. (2023). Carboxymethylcellulose/agar-based functional film incorporated with nitrogen-doped polyethylene glycol-derived carbon dots for active packaging applications. *Chemosphere*, 313, Article 137627. <https://doi.org/10.1016/j.chemosphere.2022.137627>
- Vargas-Torrico, M. F., Aguilar-Méndez, M. A., Ronquillo-de Jesús, E., Jaime-Fonseca, M. R., & von Borries-Medrano, E. (2024). Preparation and characterization of gelatin-carboxymethylcellulose active film incorporated with pomegranate (*Punica granatum* L.) peel extract for the preservation of raspberry fruit. *Food Hydrocolloids*, 150, Article 109677. <https://doi.org/10.1016/j.foodhyd.2023.109677>
- Vargas-Torrico, M. F., von Borries-Medrano, E., & Aguilar-Méndez, M. A. (2022). Development of gelatin/carboxymethylcellulose active films containing Hass avocado peel extract and their application as a packaging for the preservation of berries. *International Journal of Biological Macromolecules*, 206, 1012–1025. <https://doi.org/10.1016/j.ijbiomac.2022.03.101>
- Wang, K., Li, W., Wu, L., Li, Y., & Li, H. (2024). Preparation and characterization of chitosan/dialdehyde carboxymethyl cellulose composite film loaded with cinnamaldehyde@zein nanoparticles for active food packaging. *International Journal of Biological Macromolecules*, 261, Article 129586. <https://doi.org/10.1016/j.ijbiomac.2024.129586>
- Weiland, F., Kohlstedt, M., & Wittmann, C. (2024). Biobased de novo synthesis, upcycling, and recycling — the heartbeat toward a green and sustainable polyethylene terephthalate industry. *Current Opinion in Biotechnology*, 86, Article 103079. <https://doi.org/10.1016/j.copbio.2024.103079>
- Yang, J., Li, Y., Liu, B., Wang, K., Li, H., & Peng, L. (2024). Carboxymethyl cellulose-based multifunctional film integrated with polyphenol-rich extract and carbon dots from coffee husk waste for active food packaging applications. *Food Chemistry*, 448, Article 139143. <https://doi.org/10.1016/j.foodchem.2024.139143>
- Yin, C., Sun, Z., Yang, Y., Cui, M., Zheng, J., & Zhang, Y. (2024). Rapid in situ formation of κ-carrageenan-carboxymethyl chitosan-kaolin clay hydrogel films enriched with arbutin for enhanced preservation of cherry tomatoes. *International Journal of Biological Macromolecules*, 273, Article 132957. <https://doi.org/10.1016/j.ijbiomac.2024.132957>
- Zhang, Y., Xue, C., Xue, Y., Gao, R., & Zhang, X. (2005). Determination of the degree of deacetylation of chitin and chitosan by X-ray powder diffraction. *Carbohydrate Research*, 340(11), 1914–1917. <https://doi.org/10.1016/j.carres.2005.05.005>